ISSN 1029-9599, Physical Mesomechanics, 2024, Vol. 27, No. 3, pp. 217–228. © Pleiades Publishing, Ltd., 2024.
Russian Text © The Author(s), 2024, published in Fizicheskaya Mezomekhanika, 2024, Vol. 27, No. 1, pp. 5–19.

Different-Scale Heterogeneities in Segments of Active Faults and Their Influence on Slip Modes

V. V. Ruzhich[1]*, G. G. Kocharyan[2], A. A. Ostapchuk[2], and E. V. Shilko[3]

[1] *Institute of the Earth's Crust, Siberian Branch, Russian Academy of Sciences, Irkutsk, 664033 Russia*
[2] *Sadovsky Institute for Dynamics of Geospheres, Russian Academy of Sciences, Moscow, 119334 Russia*
[3] *Institute of Strength Physics and Materials Science, Siberian Branch, Russian Academy of Sciences, Tomsk, 634055 Russia*
** e-mail: ruzhich@crust.irk.ru*

Received June 28, 2023; revised July 19, 2023; accepted July 28, 2023

Abstract—The paper presents some multidisciplinary research results on the structure of slip surfaces in segments of tectonic faults in the Baikal region and Mongolia. The properties of subsurface (modern) and deep slickensides exposed after many-kilometer denudation of the Earth's upper crust are studied at different levels—from macroscale to nanocrystals. Other types of heterogeneities characterizing the structure of fault slip zones are also considered. The presented data indicate a heterogeneous structure of tectonic faults. Their slip zones show both low-friction regions where strong mineral phases are replaced by weak minerals and potentially unstable spots with high friction resistance. Results of the comprehensive study of geological conditions under which different-scale heterogeneities emerge in exhumed fault segments should be taken into account when developing rock mass models suitable for numerical simulation of earthquake preparation processes at the micro-, meso- and macroscales.

Keywords: earthquake, coseismic rupture, fault, slip modes, slip plane, pseudotachylites, geothermal healing

DOI: 10.1134/S1029959924030019

1. INTRODUCTION

Recent reviews [1–3, etc.] report that numerous published hypotheses and data on the structure of slip surfaces of tectonic faults and their frictional properties comply with the basic principles of physical mesomechanics. According to these principles, the geological medium is treated as a multilevel hierarchical dissipative system with self-consistent evolution of nano-, micro-, meso- and macroscopic processes [4, 5, etc.]. Until recently, physical and geological works were carried out quite independently. In laboratory and numerical experiments, physicists used geomaterial samples (often their analogues with similar properties) provided by geologists and interpreted the results based on the general ideas about processes occurring in the interior of the Earth's crust. Geologists often almost ignored the results of laboratory simulation and considered them inadequate to reality [6]. At present, things are beginning to change. There appear multidisciplinary scientific teams, which include specialists in geology, geomechanics, geophysics, tribology, and mathematical modeling, etc. Publications made by these teams contain both field and laboratory data, which allows geologists to better interpret the obtained results and physicists to determine the scale of applicability of the developed models and concepts [5–12, etc.].

One of the most important effects that determine regularities of faulting and seismic vibration emission during dynamic slips is considered to be frictional interaction of the sides of tectonic faults. This problem is extensively studied (see, for example, [3] and the references therein). Despite a variety of frictional interactions, ancient coseismic faults are usually identified by slickensides, pseudotachylytes (resulting from frictional melting), and metamorphic zones containing new minerals when studying the structure and formation conditions of exhumed geoseismic objects [8, 13, 14, etc.].

Slickensides found along tectonic faults can be defined as different-scale areas of the fault plane with slickenside flutes, slickenlines, and slickensteps resulting from high-velocity slip [15]. Interest of geologists and geophysicists in slickensides was mainly

associated with the reconstruction of the stress-strain state of blocks of the Earth's crust in a wide scale and time range [16, 17, etc.]. Meanwhile, a more detailed study of the structure, location, and formation of mineral compounds in slickensides can provide new information on natural conditions of petrophysical, thermal and physicomechanical transformations, which markedly affect slip modes and generate a wide spectrum of different-frequency vibrations.

The geological survey performed by us on tectonic faults in the Baikal region and Mongolia revealed seismogenic fault segments with subsurface (modern) and deep slickensides exposed by long-term uplifting and denudation of the crust. The present paper reports and interprets the results of a multidisciplinary different-scale study of the structure of fault slip surfaces.

2. STRUCTURAL HETEROGENEITIES OF SLIP ZONES IN TECTONIC FAULT SEGMENTS

The last two decades of investigation of deep segments of active faults exposed by denudation and deep drilling of fault zones after recent strong earthquakes have significantly added to our knowledge of the structure and composition of slip zones as well as of thermodynamic conditions at seismic focal depths [1–3]. With a certain degree of convention, several levels of structural heterogeneities can be distinguished on slip surfaces of active fault zones: nanoscopic thin films resulting from macrocrystal fragmentation during relative shear displacement of the contacting rock blocks, submillimeter geomaterial structures, centimeter-meter blocks in breccia and melange, different-sized slickenside formations, macro- and megaroughness, and waviness of slip surfaces [1–3, etc.]. Local areas of the contact surface with different frictional properties are apparently of decisive importance in building the dynamic slip model.

Under the influence of the laboratory results and the growing evidence of structural heterogeneity of slip zones, the idea of contrasting "strong" and "weak" faults [18, etc.] was transformed into the assumption of coexistence of "strong" and "weak" areas in the fault zone [9, 10, etc.]. Such ideas correspond to the well-known seismological approach, according to which the slip surface has special areas, i.e. "asperities", which present "strong, stressed" spots surrounded by areas where the stress is partially relieved during the interseismic period [19]. Strong spots have a high friction resistance according to Byerlee's law [20], while weak spots are supposedly characterized by extremely low static friction coefficients of the fault core materials [3, 10, etc.].

Common examples of macroscopic areas with different frictional properties are quartz-bearing rocks and phyllosilicate-rich regions. For example, work [21] describes the structure of exhumed basement rocks, which consists of deformation zones in interconnected phyllosilicate regions surrounding several-hundred-meter-thick quartz lenses. The latter are more or less dense clusters of lower-level asperities, which are usually nonuniformly distributed over the fault plane.

The frictional properties of fault gouge differ significantly from the properties of the host rocks. This is due to the metasomatic and metamorphic transformation of rocks during the long-term evolution of the fault core. Fillers of the fault core can be conventionally divided into two groups: (1) foliated geomaterials containing silicates (halite, talc, biotite, montmorillonite, and other phyllosilicates); (2) fillers based on such materials as quartz, granite, orthoclase, calcite, dolomite, etc. Phyllosilicates generally have a noticeably lower friction coefficient. In particular, montmorillonite with a high adsorption capacity has a friction coefficient of only 0.18 under a normal stress of 20 MPa at room temperature [3, 11]. In contrast, quartz-rich gauge has a relatively high friction coefficient. The difference in frictional properties between the quartz and phyllosilicate fillers becomes even more radical when they are saturated with fluid. Though the friction resistance of nonadsorbing minerals, such as quartz, is hardly affected by fluid saturation, the friction coefficients of such materials as montmorillonite or lizardite decrease significantly upon saturation because water-saturated minerals have a decreased strength. An even more important role in slip dynamics, as compared to the friction coefficient, is played by variations in friction resistance during shear. Areas in which dynamic slip originates must be prone to weakening. The type of fault slip depends both on the material composition of the contact zone and on the external conditions, such as pressure, temperature, presence of fluid, and slip velocity. Fillers rich in strong minerals exhibit less stable sliding than those rich in weak minerals. This is facilitated by the foliated structure of phyllosilicate minerals, as opposed to the granular structure of stronger geomaterials. However, the threshold concentration of phyllosilicate in gauge for stable sliding under different P–T conditions and slip velocity is still undetermined. The influence of various parameters on the frictional behavior of geomaterials was

discussed in detail in [3]. Friction parameters of many geomaterials composing slip zones of tectonic faults can be found in the same paper.

In seismological observations, weakening areas appear as topologically dense clusters of hypocenters of background seismicity [22]. Such clusters are the main elements that determine integral patterns of shear resistance of the fault. Hypocenters of larger events are often located near their boundaries. According to the results of [22], the shape of asperities can be approximated by an ellipse, with the axes coinciding with the main elements of topologically dense clusters of background seismicity.

Data on the size of large-scale asperities were analyzed in work [1], according to which the characteristic size of areas interpreted as asperities was on average 1.5–3 times smaller than the estimated length of seismogenic ruptures. The teleseismic data for these areas are even smaller. Thus, the characteristic asperity size is estimated to be $L \sim 25$ km for the July 17, 2017 M_w 7.8 earthquake (Commander Islands), $L \sim 14$ km for the September 08, 2021 M_w 7 earthquake (Acapulco, Mexico), and $L \sim 66$ km for the known March 11, 2011 M_w 9 event (Tohoku, Japan). With a large scatter of values, the average characteristic size of such regions is $L \sim 9.5$ km for earthquakes with the seismic moment $M_0 \sim 1019$–1020 N m, $L \sim 15$ km for $M_0 \sim 1020$–1021 N m, for $L \sim 28$ km $M_0 \sim 1021$–1022 N m [1 and the references therein]. Judging from the available data, asperities occupy about 20–30% of the rupture surface area.

2.1. Segmented Zone of the Primorsky Fault

The Primorsky normal fault follows the old suture line of the Siberian Craton. The fault segment we study actively developed in the Early Paleozoic (≈500 million years ago) [23] and in later periods, including 60–70 million years of formation of the Baikal Rift Zone [14, 24]. Within this period, the 200-km-long segment of the Primorsky rift fault was formed (Fig. 1). In the Middle Paleozoic, as a result of long-term denudation, deep layers gradually approached the Earth's surface [23]. This was accompanied by the decrease in temperatures and pressures to $T \approx 550$–350°C and $P \approx 350$–150 MPa, naturally

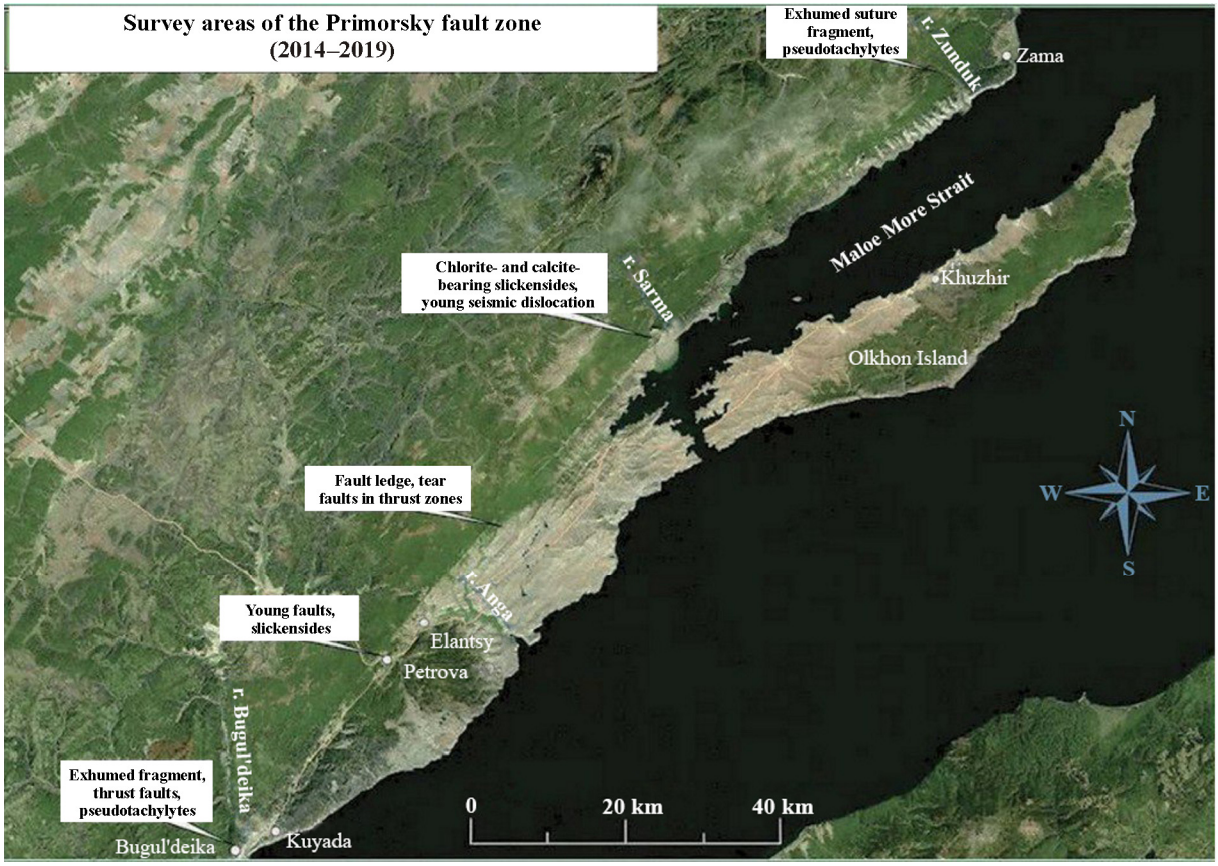

Fig. 1. Satellite image showing the location of the Primorsky fault zone and areas of detailed geological and structural survey of its segments (color online).

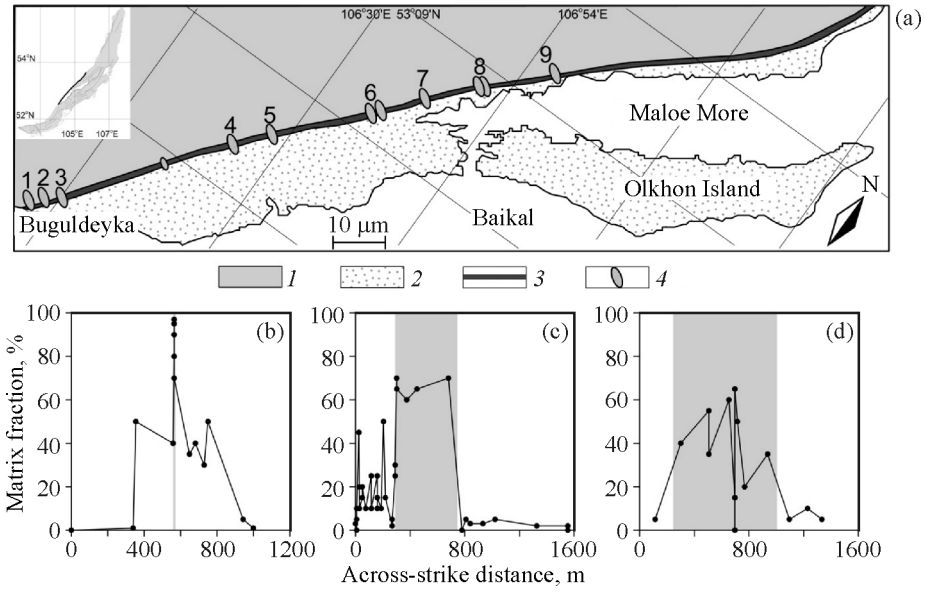

Fig. 2. Map of the Primorsky fault and types of strain localization. Location of the studied areas of the Primorsky fault: *1*—Siberian Craton, *2*—Olkhon terrain, *3*—Primorsky fault (craton-terrain collision suture), *4*—studied areas (a). Types of strain localization in the studied zones; the amplitude of accumulated strain is estimated by the fraction of the matrix in the rock (the strain localization is marked in gray): type *1*—strain localization in a narrow zone with the thickness from a few to tens of centimeters (b); type *2*—rather uniform strain distribution in a zone from hundreds of meters to a kilometer (c); type *3*—nonuniform strain distribution, weakly deformed zones can be distinguished inside the core (d).

changing rock properties by the so-called retrograde metamorphism. As a result, exhumed segments of the suture can be used for visual study of deep layers of the Earth's crust with physical and mechanical parameters characteristic of 10–20-km-deep layers. According to the present knowledge, similar *P*–*T* conditions currently exist within the Baikal Rift Zone. They correspond to the 7–20-km-deep seismic focal layer, where most of the hypocenters of modern earthquakes are located, including the strongest ones with M = 7.0–7.9 [25 and etc.].

For several years, Primorsky fault segments have been jointly investigated by specialists from the Institute of the Earth's Crust SB RAS, the Institute of Geology of Ore Deposits, Petrography, Mineralogy and Geochemistry RAS, and the Institute for Dynamics of Geospheres RAS. The result of this investigation was a digital catalog of rock samples from the Primorsky fault, including their petrographic characteristics, chemical composition, thin-section photographs, and positioning within 5 m (Fig. 2) [26, 27].

The analysis of the digital catalog demonstrated a pronounced variation in the material composition of rock samples both across and along the strike. The characteristic spatial scale of along-strike variations in frictional properties of the fault core is ~30 km. The detailed petrographic description and determination of the material composition across the strike reveal the site of the severest deformations (fault core), occurrence and frictional properties of slickenside formations, and patterns of shear strain accumulation in various segments of the fault zone. It was found that, the higher the amplitude of accumulated strain, the higher the rock refinement at the microlevel and the larger the proportion of the matrix (a fine-grained submicron-sized material that surrounds larger grains in the rock). Three types of segments with different rheological behavior were distinguished along the studied 160-km fault. In segments of the first type (Buguldeika River, Sarma River), strains are localized in a narrow zone composed of rocks that feature velocity weakening. Such segments accumulate displacements due to recurring seismic slips. Numerous dynamic slips result in a narrow mylonitized zone (fault core), where strain is maximum. It is in these segments that numerous slickensides (Fig. 3) and foci of paleoearthquakes are often found [8, 14, 28, etc.].

In segments of the second type (Anga River, Khorga River), cataclastic strains are uniformly distributed over an area several hundreds of meter thick across the strike. Materials composing the fault core in such segments are prone to velocity strengthening. This leads to strain accumulation due to aseismic slip.

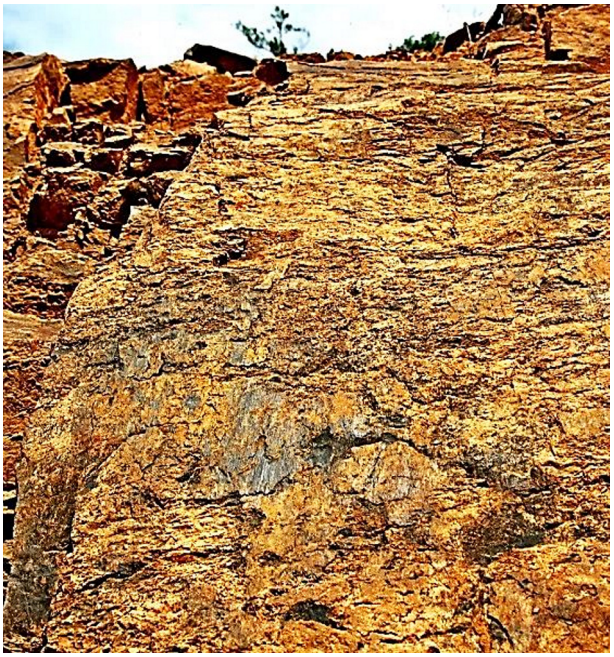

Fig. 3. Slickenside in the granite barrow pit (Petrov village) located in the Primorsky normal fault zone. Seen are subvertical slickenlines characteristic of normal faults with signs of weak chloritization as well as signs of highly intense metasomatic transformation and a thin film of frictional melting (vitrification), which indirectly indicate shallow depths of its origin, presumably during the Neogene-Quaternary period of formation of the Baikal Rift basin (photo by V.V. Ruzhich) (color online).

Segments of the third type (Talovka River, Kurma River) are characterized by a heterogeneous core structure and a mixed type of strain accumulation. The fault core includes areas composed of both rocks with velocity strengthening and velocity weakening. The structural heterogeneity of the fault core affects the slip mode and accumulated strain. Aperiodic seismic slips of different age can localize at the boundaries of competent beds, as well as at the boundary between the core and host rock.

Fig. 4. Modern slickenside in gouge formed in a seismic dislocation during the destructive Kobe earthquake on January 17, 1995 (M = 7.3) (photo courtesy of Yoshiro Kinugasa) (color online).

A more detailed examination of microscopic and nanoscopic processes of formation of slickensides provides additional information about refinement and metamorphic transformations of various rocks at depth. Melting traces in the form of a vitreous film or pseudotachylytes allow estimating thermodynamic parameters of frictional heating, sliding characteristics, and the involvement of different fluids [7, 8, etc.].

3. STRUCTURE OF SUBSURFACE SLICKENSIDES IN MODERN SEISMIC DISLOCATIONS

Structural analysis of some modern seismic dislocations reveals fresh slickensides. Figure 4 shows a photograph of a subsurface slickenside that was exposed on the rupture surface after the January 17, 1995 Kobe earthquake (Japan, moment magnitude $M_w = 7.3$). The displacement is seen to occur along the oblique slip fault in the plastic gouge, which exhibits pronounced oblique slickenlines. The direction and amplitude of displacements can be easily determined by the displacement of the fault walls.

Similar, but larger, slickensides were formed in the Upper Paleozoic loose clay sediments during the December 4, 1957 Gobi-Altai earthquake (M = 8.1). The survey performed in 1958 for a 275 km segment of the modern seismic dislocation of this event revealed a slickenside. The resulting coseismic rupture had a left-lateral oblique slip displacement with the amplitude 4–8 m, and the earthquake intensity was 11 [14, 29]. In the first years, fresh minerals retained wave-like slickenlines in the left-lateral oblique slip direction with the amplitude 3.5 m (Fig. 5) [29].

From the experience of field studies of subsurface slickensides formed in seismic dislocation zones at low pressures, slip traces in the form of slickensides remain only in loose sediments. Solid rocks have no pronounced slickenlines on asperities coming in contact at low pressures. Thus, the study of subsurface slickensides yields little information in contrast to deep slickenside.

4. STRUCTURE OF EXHUMED DEEP SLICKENSIDES

Uplifting of deep layers of the Earth's crust during geological evolution and denudation processes provides access to segments of ancient faults which

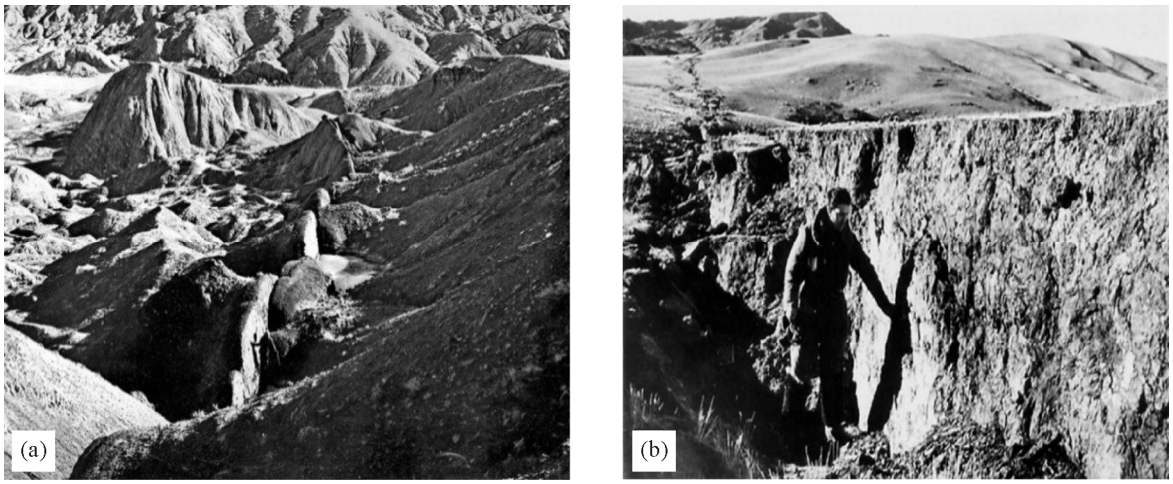

Fig. 5. Seismic dislocation zones of the 1957 Gobi-Altai earthquake: the Khutusuj tract in southern Mongolia where the Soviet-Mongolian expedition discovered one of the most dramatic seismic dislocations in 1958 (a); slickenside in this seismic dislocation, near which you can see the leader of the expedition V.P. Solonenko, corresponding member of the Academy of Sciences of the USSR [29] (b).

were active in the past seismic tectonic periods. Millions of years ago, these rock masses were located at the depths 10–15 km. According to [30], the rate of exhumation of one of deep segments of the San Andreas Fault was estimated to be about 0.225 mm/year. A thorough examination reveals various characteristic traces of dynamic slips, including slickensides with signs of frictional melting of rocks. Similar formations were found in exhumed segments of paleoearthquake foci concentrated along the suture line of the Siberian Craton and in deep faults in the northern and central Mongolia [7, 14].

4.1. Collision Suture of the Siberian Craton and Its Primorsky Segment

Now let us discuss the results of investigation of deep slickensides in the Baikal region. One of the studied objects (rock exposure) is located at the mouth of the Bolshaya Buguldeika River flowing into Lake Baikal. Its geoposition is associated with the exhumed segment of the collision suture of the Siberian Craton, which includes the above-described segment of the seismogenic Primorsky fault. Field studies of this segment in 2014–2022 revealed signs of coseismic ruptures of paleoearthquakes with deep slickensides (Fig. 6) [7].

One of the distinct features of the exhumed segment of the deep seismic focal layer of the Earth's crust is the prevalence of tourmaline mineralization. It apparently formed in the temperature range 550–350°C due to hydrothermal fluids ejected from igneous boron-rich granite formations. The identified signs of coseismic slips in the form of slickensides and tourmaline mineralization suggest that the tem-

Fig. 6. Northeastern segment of the suture of the Siberian Craton (az. 50°–60°) and structure of deep slickensides on different scales: a—exhumed Primorsky segment of the suture zone containing signs of elements of paleoearthquake foci (left bank at the mouth of the Bolshaya Buguldeika River), the arrow indicates the location of a deep slickenside sample with tourmaline mineralization; b—photo of the slickenside with tourmaline mineralization; c—polished section of the tourmaline-coated slickenside with signs of plastic deformations and discontinuities of the tourmaline layer (color online).

perature conditions of dynamometamorphism correspond to the rheology of brittle-plastic transition at the depths 10–15 km.

Estimating the absolute age of ancient deep coseismic ruptures is a separate complex task associated with the identification of "geochronometer" minerals [31]. For this purpose, use was made of a rare mineral, namely, tourmaline of metasomatic genesis (the process of almost simultaneously replacement of old minerals by new ones so that mineral complexes keep solid throughout the replacement process), whose petrochemical and physical properties ensure high resistance to induced thermal influences. The found slickensides with tourmaline mineralization allow its age dating. A detailed study of thin sections (Fig. 6c) showed that, despite a high hardness (7 on the Mohs scale) and melting point, tourmaline on slickensides of coseismic ruptures exhibited clear signs of viscoplastic flow. This gives reason to believe that this type of rheological behavior of the tourmaline coating with slickenlines occurred in deep P–T conditions. The absolute age of tourmaline mineralization in coseismic ruptures with slickensides in the vicinity of the sources of the Bolshaya Buguldeika River was estimated to be 673 ± 5 mln years [8]. The coseismic slip evidenced by the mineral composition of the slickenside coating is most likely younger than the absolute age of the tourmaline layer.

Another important indicator of deep coseismic ruptures are pseudotachylytes [14, 32, 33, etc.]. These glassy formations, which are similar to volcanic glass, generated under conditions of high-amplitude dynamic slips during frictional heating in fault zones. Such formations were discovered in the Baikal region among cracks of mylonitized granites and granodiorites of the Primorsky complex. Pseudotachylytes most often occur as thin branching veins 1–2 mm to 5 cm wide in mylonitized rock. From thin sections it is seen that their initial state was almost completely changed under conditions of severe cataclasis and mylonitization.

Thermodynamic conditions during paleoearthquakes can be estimated using the so-called geothermometers and geobarometers, whose parameters can be used to determine thermodynamic conditions and consequently the depth of the studied processes. These methods are based on the ideas of P–T dependences of the equilibrium constants of crystalline rock minerals [31, 34]. According to the performed calculations, the temperature and pressure reached $T \sim 850$–950°C and $P \sim 500$–550 MPa in pseudotachylytes. The derived petrochemical pattern was interpreted as the result of dynamic slip along faults, during which pressure and temperature increased locally by $\Delta P \sim 200$–250 MPa and $\Delta T \sim 450$–500°C above the initial level [35]. Additional evidence for such high pressures can be the presence of such mineral as barroisite in pseudotachylytes, which is considered characteristic of high-pressure metamorphic complexes [36].

Instead of pseudotachylite veins, many deep slickensides contain thin vitreous films, which also indicate high-velocity slip along coseismic faults.

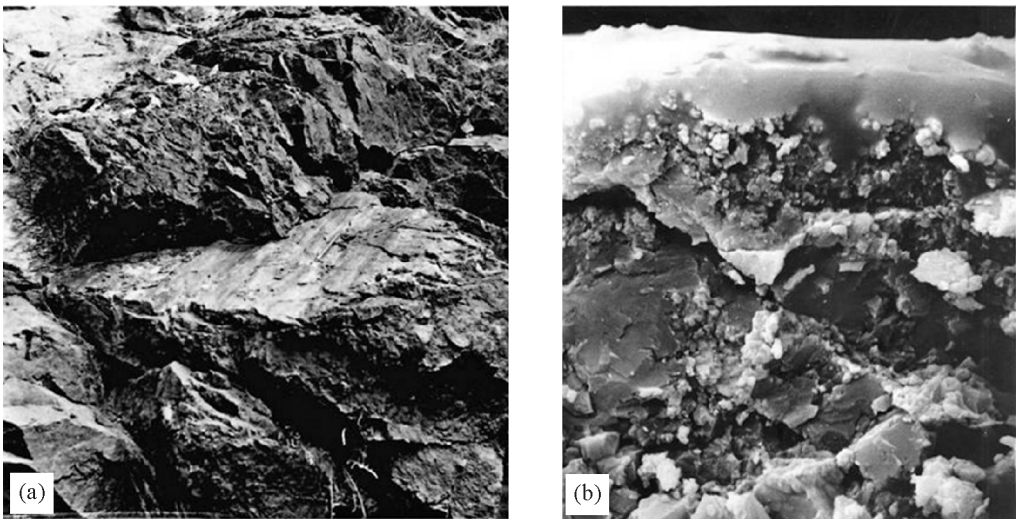

Fig. 7. Sample of a deep slickenside from a segment of the Bogd fault (Mongolia): a—general view of the slickenside in the Bogd fault segment in the vicinity of Lake Orog Nurr; b—electron microscopy of the slickenside sample with a thin vitreous film formed due to frictional heating during coseismic sliding [14, 37].

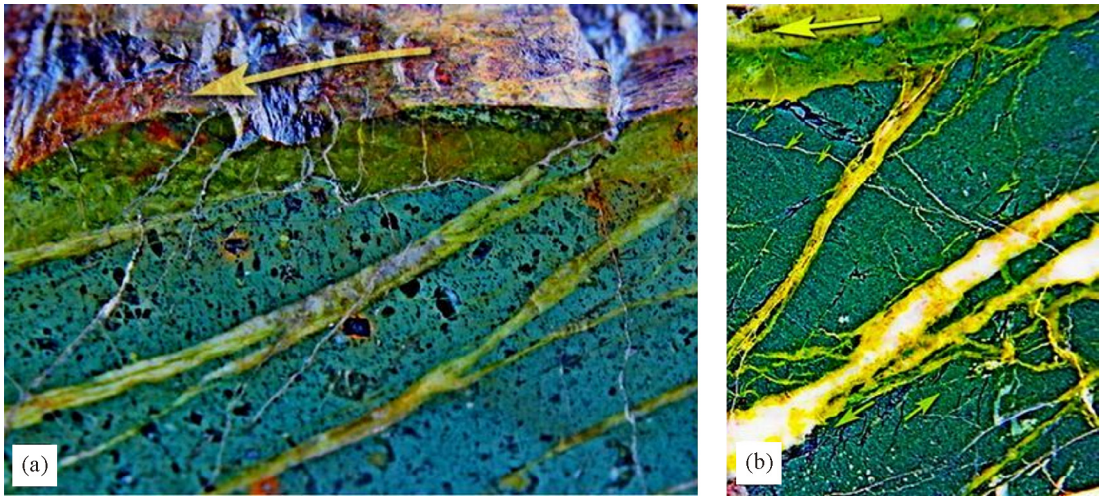

Fig. 8. Polished section of a deep slickenside formed in andesite from a segment of the Bodg fault (Mongolia): a—polished section of a vitreous slickenside in the andesite sample, the arrow at the top indicates the direction of coseismic slip [14, 37]; b—enlarged fragment, where arrows show the slip direction and en echelon tension fractures along the en echelon fault (color online).

4.2. Bogd Fault Zone in Mongolia

A sample of deep slickensides was taken from the seismic dislocation zone in the Bogd fault segment in the Gobi Altai region, where the above-mentioned large earthquake with M = 8.1 occurred on December 4, 1957 (Fig. 7) [14, 29, etc.]. Figure 8 shows a polished section of the deep slickenside from this zone, where a vitreous slip surface with slickensteps is visible. This rock sample is composed of minerals (epidote, albite, etc.) corresponding to the greenschist facies of metamorphism ($T < 500$°C). The paragenesis of minerals (albite + epidote) newly formed in this sample indicates that its multistage deformation occurred in the presence of the fluid with a high concentration of Na+ ions and a low concentration of CO_2, as indicated by the stability of epidote and the absence of calcite. The conditions of frictional heating, melting of a finely ground geomaterial, and the formation of a vitreous film were realized in such deep fault segments at the slip velocity of the order of 1–10 m/s.

It is important to note that slip planes and inclined en echelon fractures had quartz-chlorite mineralization and calcite precipitated from fluids of the corresponding chemical composition. It can be assumed that such fluids are injected into the vacuum space of opening tensile fractures under high pressure and speed. According to petrographic analysis, quartz deposits form under severe deformation. According to the existing petrochemical models, such fluidization phenomena in the considered slickenside formations apparently occurred under the corresponding *P–T* conditions of the greenschist facies of metamorphism at the seismic focal depths 5–8 km [8].

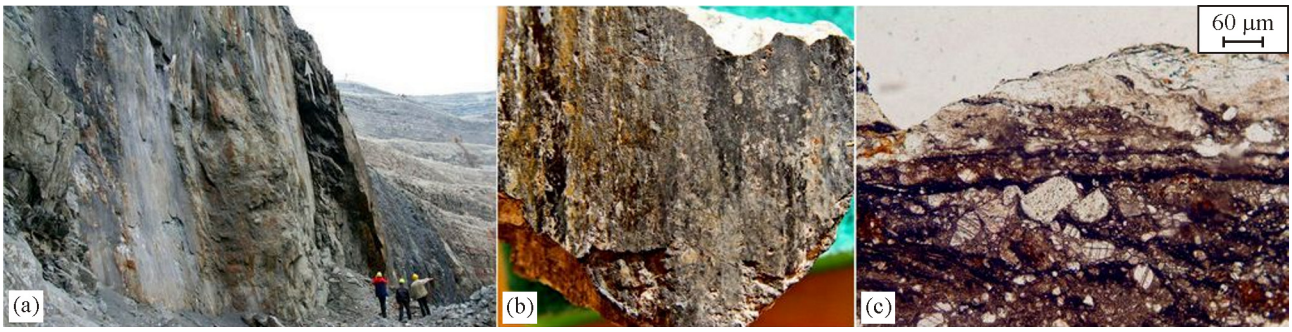

Fig. 9. Different-scale heterogeneities from a segment of the Vilyui fault zone (az. 50°–60° NE): a—one of the large-scale slickensides in the ultradeep Udachny mine exposed at the depth 475 m; b—slip surface fragment containing a slickenside; c—polished section of the slickenside shown in Fig. 9b with two slip planes formed in different periods of coseismic slips (color online).

4.3. Slickensides in the Ultradeep Udachny Mine

The mine is located in the vicinity of the Udachnaya diamond pipe in the Sakha Republic (Yakutia). Figures 9a and 9b show a Vilyui fault segment with numerous slickensides, which was exposed by excavation of the diamond explosion pipe in the ultradeep Udachny mine. Figure 9a exhibits a general view of the slickenside whose sample is presented in Fig. 1. Figure 9c presents a section cut perpendicular to the slip plane, where another two older slip planes are seen dark.

A dolomitic sediment layer containing the discovered fragment was formed in the interval 445–485 mln years. Judging from the mineral coating, the slickenside was formed at the temperature $T = 350$–450°C and the pressure $P = 200$–400 MPa, which corresponds to the depth 5–8 km.

This slickenside sample was studied in great detail using X-ray scattering methods, infrared and fluorescence spectroscopy [38], which gave a number of qualitatively new results. In particular, it was found that the slickenside has a shiny nonuniformly vitrified film with slickenlines. Its surface layer 30 nm thick is composed mainly of quartz and albite nanocrystals with a large number of defects such as broken interatomic bonds and impurity ions. Nanocrystals have water on the surface. The 2–4-μm-thick layer of the slickenside contains nanocrystals of albite, quartz, calcite, and dolomite. Minerals in the slickenside plane experienced intense transformations. Quartz nanocrystals have the size ≈19 nm. Their lattices are compressed to ≈0.6%, which corresponds to the effective lattice compression stress ≈0.23 GPa. At the same time, quartz crystals in the rock under the slickenside have macrosizes. Nanocrystals are assumed to be formed from macrocrystals fragmented during the relative shear movement of the contacting rock blocks. The presence of water reduces the activation energy of SiOSi bond breaking, which contributes to unstable strike slip with the formation of a slickenside. Water can also destruct albite and quartz crystals by hydrolysis [39]. Such a structure decreases the friction coefficient and creates conditions for unstable slip. Apparently, this is a typical structure of slickensides. For example, the surface layer of the slickenside sample taken from the seismic dislocation of the 1957 Gobi-Altai earthquake consists mainly of deformed nanocrystals of epidote (aluminosilicate with a low friction coefficient) and water [40]. A nanoscopic study of a slickenside formed in sandstone revealed deformed nanocrystals of montmorillonite (a typical product of aluminosilicate weathering) and anatase in its composition [41].

5. RESULTS AND DISCUSSION

The results reported in this paper point to a pronounced hierarchy of heterogeneities in the structure and properties of the slip surface of tectonic faults.

The highest hierarchical level is presented by large heterogeneities with an area approximately an order of magnitude smaller than the area of earthquake foci. They are contact spots governed by the complex topography of the slip surface. It is these asperity contacts (stress concentration zones) that turn out to be dynamically unstable during sliding along the fault, while fault areas between the contacting asperities have frictional properties of stable sliding. This is due to the formation of quartz- and feldspar-rich areas in the contact spots, which almost lack phyllosilicates. Minerals transported by fluids are sedimented between the contacting asperities with the formation of interlayers of weak phyllosilicate-rich materials, i.e. surface areas with frictional properties of velocity strengthening.

In geodetic observations, areas of large-scale asperities can be clearly identified as a deficiency of interseismic events. These areas are often characterized by seismic quiescence. The latter is usually considered as one of the intermediate precursors of earthquakes. Smaller contact spots appear as topologically dense clusters of hypocenters of background seismicity.

The next level is local slip zones. They are found on exhumed surfaces or in drill cores in the form of slickensides and pseudotachylytes. Structural analysis and laboratory experiments of these formations provide valuable information about the P–T conditions of preparation of coseismic ruptures in earthquake foci and about processes during sliding. For example, it is often assumed that fault gouge forms at relatively small depths (above the lower boundary of the greenschist facies, $T < 250$–350°C) in a brittle region due to frictional wear and cataclastic deformations (grain boundary sliding, grain cracking, etc.). At the same time, the mineralization of fracture surfaces and slickensides of the Primorsky fault indicates that the most ancient coseismic ruptures with slickensides occurred under P–T conditions of the amphibolite facies of metamorphism (pressure 0.7–1.0 GPa, temperature 500–700°C). This result is consistent with the data of the recent laboratory experiments, which significantly expanded the range of

P–T conditions of quasi-brittle fracture. In particular, it was shown that dynamic slips in calcite gouge could occur at such high temperatures as 550°C. At the same time, thin sections of samples fractured by a brittle mechanism showed a characteristic mylonite microstructure (elongated grains, aligned elongated porphyroclasts, recrystallization) [42]. It was reported in [43] that the presence of quartz provided a local increase in high stresses, which caused the refinement and destruction of crystals in minerals with weaker atomic bonds (feldspars and micas) and the formation of a nanocrystalline, partially amorphous, material, which facilitated sliding. Shear tests on a mafic rock layer under very high pressures (compressive pressure $0.5\ \text{GPa} \le P_c \le 1.5\ \text{GPa}$) at the temperature 600°C revealed a predominantly brittle deformation mechanism, with the transition to viscous deformation at the temperature 800°C [44]. The authors of [43] related quasi-brittle fracture at high pressures and temperatures to micro- and nanoscopic structural heterogeneities. They suggested that the partially amorphous material generated by solid-state amorphization formed a weakening area penetrating the mylonitized rock layer, and the high stress concentration at the interface between the slip zone and the host rock caused brittle fracture of the fault [43].

Within the rate-and-state friction (RSF) rheology commonly used in the description of fault sliding, the possibility of dynamic slip is determined by the relation between the rigidity of the host rock and the rate of decrease in the shear resistance during fault sliding [3]. Various modifications of the RSF model are employed to simulate numerous natural phenomena associated with fault sliding [2 and the references therein], including slow events. The conventional RSF model allows simulating these phenomena only in a very narrow parameter range [2], which contradicts the latest observational data, according to which slow events often occur at various crustal depths [45]. The recent numerical simulation [46] demonstrated that consideration for the dependence of the RSF parameters on the displacement velocity of the fault sides significantly expanded both the range of conditions in which slow events can occur, and the range of their characteristics, such as released stresses, duration, and recurrence.

Heterogeneities of the smallest hierarchical level—nanolevel—were directly detected in the mentioned experiments, in which the slickenside structure was studied by X-ray scattering methods, infrared, fluorescence and molecular spectroscopy [38, 40, 41]. These experiments were first to show that frictional contact of rocks under high pressure resulted in a radical transformation of the material structure associated with the fragmentation of macrocrystals in a very thin layer. In combination with other processes, for example, pronounced water flooding, these effects can cause a critical decrease of friction in the contact area and coseismic slip.

The information obtained for different-scale heterogeneities in fault segments, their geometry, the role of fluids on different scales, morphology and strength properties of asperities at the sites of coseismic ruptures is expected to be in demand for reconstruction of earthquake preparation conditions. In recent years, slip models with different consideration for the fault structure heterogeneity began to appear [1, 10, 47, 48, etc.].

6. CONCLUSIONS

Many years of experience in field geological and structural studies indicate the possibility of identifying paleoseismogenic objects in fault zones by certain features which became accessible for visual examination after long-term many-kilometer denudation of the upper layers of the uplifted Earth's crust.

The reported data bear witness to a heterogeneous structure of tectonic faults. Their slip zones include low-friction regions, where fluid saturation promotes weakening of strong mineral phases and whose friction increases with increasing slip velocity, and high-friction regions where deformation is predominantly cataclastic. The petrochemical and structural analysis of deep slickensides revealed that they can be used for identification of coseismic ruptures formed at the seismic focal depth in periods of seismic activations. The derived data also provide substantiated evidence for thermodynamic conditions of formation of coseismic ruptures.

The data of the comprehensive study of geological conditions of emergence of different-scale heterogeneities on exhumed fault segments will undoubtedly contribute to the construction of more acceptable complex rock models for numerical simulation of formation of high-grade dangerous earthquake foci.

FUNDING

The research by V.V. Ruzhich was carried out within the government statement of work for the Institute of the Earth's Crust SB RAS (research line FWEF-2021-0009) using the equipment and infrastructure of the Geodynamics and Geochronology CUC IEC SB RAS under grant No. 075-15-2021-

682. The collection and storage of samples was partially supported by government statement of work for the Sadovsky Institute for Dynamics of Geospheres RAS (research line 122032900178-7). Research by G.G. Kocharyan and A.A. Ostapchuk was financially supported by the Russian Science Foundation, grant No. 22-17-00204.

CONFLICT OF INTEREST

The authors of this work declare that they have no conflicts of interest.

REFERENCES

1. Kocharyan, G.G. and Kishkina, S.B., The Physical Mesomechanics of the Earthquake Source, *Phys. Mesomech*., 2021, vol. 24, no. 4, pp. 343–356. https://doi.org/10.1134/S1029959921040019
2. Kocharyan, G.G., Nucleation and Evolution of Sliding in Continental Fault Zones under the Action of Natural and Man-Made Factors: A State-of-the-Art Review, *Izv. Phys. Solid Earth*, 2021, vol. 57, no. 4, pp. 439–473.
3. Kocharyan, G.G., Besedina, A.N., Gridin, G.A., Morozova, K.G., and Ostapchuk, A.A., Friction as a Factor Determining the Radiation Efficiency of Fault Slips and the Possibility of Their Initiation. State of the Art, *Izv. Phys. Solid Earth*, 2021, vol. 59, no. 3, pp. 337–363.
4. Panin, V.E., Egorushkin, V.E. and Panin, A.V., Physical Mesomechanics of a Deformed Solid as a Multilevel System. I. Physical Fundamentals of the Multilevel Approach, *Phys. Mesomech*., 2006, vol. 9, no. 3–4, pp. 9–20.
5. Panin, V.E. and Egorushkin, V.E., Deformable Solid as a Nonlinear Hierarchically Organized System, *Phys. Mesomech*., 2011, vol. 14, no. 5–6, pp. 207–223.
6. Gufeld, I.L., *Seismic Hazard. To Prevent or Warn*, Moscow: Sam Polygraphist LLC, 2019.
7. Ruzhich, V.V. and Kocharyan, G.G., On the Structure and Formation of Earthquake Sources in the Faults Located in the Subsurface and Deep Levels of the Crust. Part I. Subsurface Level, *Geodin. Tektonofiz.*, 2017, vol. 8, no. 4, pp. 1021–1034. https://doi.org/10.5800/GT-2017-8-4-0330
8. Ruzhich, V.V., Kocharyan, G.G., Savelyeva, V.B., and Travin, A.V., On the Structure and Formation of Earthquake Sources in the Faults Located in the Subsurface and Deep Levels of the Crust. Part II. Deep Level, *Geodin. Tektonofiz.*, 2018, vol. 9, no. 3, pp. 1039–1061. https://doi.org/10.5800/GT-2018-9-3-0383
9. Kocharyan, G.G. and Batukhtin, I.V., Laboratory Studies of Slip along Faults as a Physical Basis for a New Approach to Short-Term Earthquake Prediction, *Geodin. Tektonofiz.*, 2018, vol. 9, no. 3, pp. 671–691. https://doi.org/10.5800/GT-2018-9-3-0367
10. Collettini, C., Tesei, T., Scuderi, M.M., Carpenter, B.M., and Viti, C., Beyond Byerlee Friction, Weak Faults and Implications for Slip Behavior, *Earth Planet. Sci. Lett*., 2019, vol. 519, pp. 245–263. https://doi.org/10.1016/j.epsl.2019.05.011
11. Ikari, M.J., Marone, C., and Saffer, D.M., On the Relation between Fault Strength and Frictional Stability, *Geology*, 2010, vol. 39, no. 1, pp. 83–86. https://doi.org/10.1130/G31416.1
12. Popov, V.L., *Contact Mechanics and Friction. Physical Principles and Applications*, Springer-Verlag GmbH, 2017. https://doi.org/10.1007/978-3-662-53081-8
13. Sibson, R.H., Fault Rocks and Fault Mechanisms, *J. Geol. Soc*., 1977, vol. 133, pp. 191–213. https://doi.org/10.1144/gsjgs.133.3.0191
14. Ruzhich, V.V., *Seismotectonic Destruction in the Crust of the Baikal Rift Zone*, Novosibirsk: SB RAS Publ. House, 1997.
15. *Glossary of Geology*: *in 3 vols.*, vol. 1, Petrov, O.V., Ed., St. Petersburg: VSEGEI Publ. House, 2010.
16. Ruzhich, V.V. and Ryazanov, G.V., On Slickensides and Mechanism of Their Formation, in *Mechanisms of Formation of Tectonic Structures of Eastern Siberia*, Novosibirsk: Nauka, 1977, pp. 105–108.
17. Rebetsky, Yu.L., Sim, L.A., and Marinin, A.V., *From Slickensides to Tectonic Stresses. Methods and Algorithms*, Leonov, Yu.G., Ed., Moscow: GEOS Publ. House, 2017.
18. Lachenbruch, A.H. and Sass, J.H., The Stress Heat-Flow Paradox and Thermal Results from Cajon Pass, *Geophys. Res. Lett*., 1988, vol. 15, no. 9, pp. 981–984. https://doi.org/10.1029/gl015i009p00981
19. Kanamori, H. and Stewart, G.S., Seismological Aspects of the Guatemala Earthquake of February 4, 1976, *J. Geophys. Res. Solid Earth. B*, 1978, vol. 83, no. 7, pp. 3427–3434. https://doi.org/10.1029/JB083iB07p03427
20. Byerlee, J., Friction of Rocks, *Pure Appl. Geophys*., 1978, vol. 116, pp. 615–626. https://doi.org/10.1007/BF00876528
21. Volpe, G., Pozzi, G., Carminati, E., Barchi, M.R., Scuderi, M.M., Tinti, E., Aldega, L., Marone, C., and Collettini, C., Frictional Controls on the Seismogenic Zone: Insights from the Apenninic Basement, Central Italy, *Earth Planetary Sci. Lett*., 2022, vol. 583. https://doi.org/10.1016/j.epsl.2022.117444
22. Kocharyan, G.G. and Ostapchuk, A.A., Mesostructure of a Tectonic Fault Slip Zone, *Phys. Mesomech*., 2023, vol. 26, no. 1, pp. 82–92. https://doi.org/10.1134/S1029959923010095
23. Donskaya, T.V., Bibikova, E.V., Mazukabzov, A.M., Kozakov, I.K., Gladkochub, D.P., Kirnozova, T.I., Plotkina, Yu.V., and Reznitsky, L.Z., The Primorsky Granitoid Complex of Western Cisbaikalia: Geochronology and Geodynamic Typification, *Geolog. Geophys.*, 2003, vol. 44, no. 10, pp. 968–979.
24. Lunina, O.V., Gladkov, A.S., and Cheremnykh, A.V., Fracturing in the Primorsky Fault Zone, *Geolog. Geophys.*, 2002, vol. 43, no. 5, pp. 446–455.
25. Radziminovich, Ya.B., Filippova, A.I., Gileva, N.A., and Melnikova,V.I., Earthquake of February 3, 2016 in the Middle Baikal Region: Source Parameters and Macroseismic Effects, *Izv. Atmos. Ocean. Phys.*, 2022, vol. 58, no. 8, pp. 936–953. https://doi.org/10.1134/S0001433822080035

26. Gridin, G.A., Grigor'eva, A.V., Ostapchuk, A.A., Cheremnykh, A.V., and Bobrov, A.A., On the Structural and Material Heterogeneity of the Zone of Tectonic Discontinuity Localization, *Dinam. Prots. Geosf.*, 2023, vol. 15(1), pp. 11–22. https://doi.org/10.26006/29490995_2023_15_1_11
27. Smekalin, O.P., Chipizubov, A.V., and Imaev, V.S., Palaeoearthquakes in the Pribaikalie: Methods and Results of Dating, *Geodin. Tektonofiz.*, 2010, vol. 1, no. 1, pp. 55–74. https://doi.org/10.5800/GT-2010-1-1-0006
28. Ruzhich, V.V., Tectonic Creep in Zones of Seismically Active Faults in the Baikal Region and Mongolia, in *Lithosphere of Central Asia*, Novosibirsk: Nauka, 1996, pp. 123–128.
29. Solonenko, V.P., Gobi-Altai Earthquake, *Geolog. Geofiz.*, 1960, no. 2, pp. 3–27.
30. Boullier, A.M., Ohtani, T., Fujimoto, K., Ito, H., and Dubois, M., Fluid Inclusions in Pseudotachylytes from the Nojima Fault Japan, *J. Geophys. Res. Solid Earth. B*, 2001, vol. 106(10), pp. 21965–21977. https://doi.org/10.1029/2000JB000043
31. Ridolfi, F., Renzulli, A., and Puerini, M., Stability and Chemical Equilibrium of Amphibole in Calc-Alkaline Magmas: An Overview, New Thermobarometric Formulations and Application to Subduction-Related Volcanoes, *Contrib. Mineral. Petrol*., 2010, vol. 160, pp. 45–66.
32. Matveev, M.A., Smulskaya, A.I., and Morozov, Yu.A., Features of Frictional Melting of Rocks and Melt Crystallization in a Seismic Process: Case Study of Pseudotachylytes of the Ladoga Region, *Izv. Phys. Solid Earth*, 2022, vol. 58, no. 6, pp. 902–928.
33. Morozov, Yu.A., Bukalov, S.S., and Leites, L.A., Mechanochemical Transformations of Shungite in the Dynamic Slip Zone, *Geofiz. Issled.*, 2016, vol. 17, no. 2, pp. 5–18.
34. Perchuk, L.L., Methods of Thermometry and Barometry in Geology, *Priroda*, 1983, no. 7, pp. 88–97.
35. Ruzhich, V.V., Savel'eva, V.B., Rasskazov, S.V., Yasnygina, T.A., Kocharyan, G.G., Ostapchuk, A.A., Travin, A.V., and Yudin, D.S., Determination of the PT Conditions that Accompanied a Seismogenic Slip along a Deep Segment of the Marginal Suture of the Siberian Craton, *Dokl. Earth Sci.*, 2018, vol. 481, no. 2, pp. 1017–1020. https://doi.org/10.31857/S086956520001774-4
36. Bucher, K. and Frey, M., *Petrogenesis of Metamorphic Rocks: Complete Revision of Winkler's Textbook*, Berlin–Heidelberg: Springer-Verlag, 1994.
37. Ruzhich, V.V., Geological Approach to the Study of Paleoearthquake Sources, in *Experimental and Numerical Methods in Earthquake Source Physics*, Sadovsky, M.A., Ed., Moscow: Nauka, 1989, pp. 68–78.
38. Sobolev, G.A., Vettegren', V.I., Mamalimov, R.I., Shcherbakov, I.P., Ruzhich, V.V., and Ivanova, L.A., A Study of Nanocrystals and the Glide-Plane Mechanism, *J. Volcanol. Seismol.*, 2015, vol. 9, no. 3, pp. 151–161.
39. Bernstein, V.A., *Mechanohydrolytic Processes and Strength of Solids*, Leningrad: Nauka, 1987.
40. Sobolev, G.A., Vettegren, V.I., Ruzhich, V.V., Kirienkova, S.M., Smulskaya, A.I., Mamalimov, R.I., and Kulik, V.B., Study of Slickenside Nanocrystals from a Seismic Dislocation Zone, *Geofiz. Issled.*, 2015, vol. 16, no. 4, pp. 5–14.
41. Sobolev, G.A., Kireenkova, S.M., Morozov, Yu.A., Smulskaya, A.I., Vettegren, V.I., Kulik, V.B., and Mamalimov, R.I., Study of Nanocrystals in the Dynamic Slip Zone, *Izv. Phys. Solid Earth*, 2012, vol. 48, no. 9/10, pp. 684–692.
42. Verberne, B.A., Niemeijer, A.R., De Bresser, J.H.P., and Spiers, C.J., Mechanical Behavior and Microstructure of Simulated Calcite Fault Gouge Sheared at 20–600°C: Implications for Natural Faults in Limestones, *J. Geophys. Res. Solid Earth*., 2015, vol. 120, no. 12, pp. 8169–8196. https://doi.org/10.1002/2015JB012292
43. Pec, M., Stünitz, H., Heilbronner, R., and Drury, M., Semi-Brittle Flow of Granitoid Fault Rocks in Experiments, *J. Geophys. Res. Solid Earth*., 2016, vol. 121, no. 3, pp. 1677–1705. https://doi.org/10.1002/2015JB012513
44. Marti, S., Stünitz, H., Heilbronner, R., Plümper, O., and Drury, M., Experimental Investigation of the Brittle-Viscous Transition in Mafic Rocks—Interplay between Fracturing, Reaction, and Viscous Deformation, *J. Struct. Geology*, 2017, vol. 105, pp. 62–79. https://doi.org/10.1016/j.jsg.2017.10.011
45. Bürgmann, R., The Geophysics, Geology and Mechanics of Slow Fault Slip, *Earth Planet. Sci. Lett*., 2018, vol. 495, pp. 112–134. https://doi.org/10.1016/j.epsl.2018.04.062
46. Im, K., Saffer, D., Marone, C., and Avouac, J.P., Slip-Rate-Dependent Friction as a Universal Mechanism for Slow Slip Events, *Nat. Geosci*., vol. 13, no. 10, pp. 705–710. https://doi.org/10.1038/s41561-020-0627-9
47. Verberne, B.A., van den Ende, M.P.A., Chen, J., Niemeijer, A.R., and Spiers, C.J., The Physics of Fault Friction: Insights from Experiments on Simulated Gouges at Low Shearing Velocities, *Solid Earth*., 2020, vol. 11, pp. 2075–2095. https://doi.org/10.5194/se-11-2075-2020
48. Kocharyan, G.G., Budkov, A.M., and Kishkina, S.B., Effect of Slip Zone Structure on Earthquake Rupture Velocity, *Phys. Mesomech*., 2022, vol. 25, no. 6, pp. 549–556. https://doi.org/10.1134/S1029959922060078